



Experimental Investigation on Corrosion Control of 13Cr L80 Steel in Hydrochloric Acid Solution using Thiophene Methanol

Rajeev P. ^{*1}, Surendranathan A.O. ², Murthy Ch. S.N. ³, John Berchmans L. ⁴

^{1&2} Department of Metallurgical and Materials Engineering, ³ Department of Mining Engineering, NITK, Surathkal, Mangalore-575025, Karnataka, India

⁴ CSIR-Central Electro-Chemical Research Institute, Karaikudi 630006, T.N, India

Received 23 May 2013, Revised 13 Nov 2013, Accepted 13 Nov 2013

* Corresponding author. E mail: puthalathkanuur@yahoo.co.in; Tel : +91 8547519386

Abstract

The influence of different eco-friendly inhibitors on the corrosion behavior of 13Cr L80 steel in 15% HCl solution was experimentally investigated. In the preliminary study, corrosion tests were performed with various oil well steels like 13Cr L80, L80, N80 and P110 steels in order to evaluate the comparative corrosion resistance of these metals when exposed to 15% aqueous hydrochloric acid solutions without inhibitors. In this paper the inhibitive action of a selected inhibitor, thiophene methanol (TML) on the corrosion behaviour of 13Cr L80 steel in 15% HCl solution at different levels of concentrations (0-100 mM) was investigated using weight-loss, electrochemical polarization and AC impedance spectroscopic methods and their results were compared. The inhibition efficiency of TML increased almost linearly with its concentration and was found to be maximum (86.79%) at 75 mM and the increase in temperature resulted in the decrease of the inhibitor efficiency (η) and degree of surface coverage (θ). Surface morphology of the corroded sample was analyzed by SEM. FT-IR spectral study and TGA were carried out to characterize the surface products. The result shows that TML is a good inhibitor for 13Cr L80 steel in HCl acid medium. The adsorption of the TML on the 13Cr L80 steel surface obeyed the Langmuir adsorption isotherm. Thermodynamic and activation parameters are discussed.

Keywords: 13Cr L80 steel, corrosion inhibitors, thiophene methanol, acidization, 15% HCl.

1. Introduction

Search for new inhibitors for oil well stimulation needs more investigative attention on the evaluation of inhibitive performance of eco-friendly non-toxic organic inhibitors on oil well steels. HCl is the most difficult acid of the common acids to handle from the standpoint of corrosion. Even though various studies have been conducted on N80 steels, studies related with 13Cr L80 steel are very much limited. Usually, organic compounds exert a significant influence on the extent of adsorption on the metal surface and therefore can be used as effective corrosion inhibitors. The known hazardous effects of most synthetic organic inhibitors and restrictive environmental regulations have now made researchers to focus on the need to develop cheap and environmentally benign natural products as corrosion inhibitors [1,2]. However, although organic corrosion inhibitors have revealed sufficient effectiveness on protection of low alloy steel tubing during oil well stimulation operations, they have not provided satisfactory results for high chromium stainless steel. Corrosion resistant alloys, such as 13Cr and 22Cr stainless steel, have proven to be more susceptible to corrosive attack of hydrochloric acid used in acidization stimulation operations especially at temperatures above 65°C than low alloy steels [3]. Corrosion resistant alloys have increasingly been used for piping, pumps and valves in the production of oil and gas in the last two decades. Tubes made with 13% chromium (13Cr) are the least expensive corrosion resistant alloy (CRA) tubes that can be used to combat CO₂ corrosion and H₂S environmental cracking.

Compounds containing nitrogen, oxygen, sulphur and phosphorous have particularly been reported as efficient corrosion inhibitors. These compounds can adsorb on the steel surface blocking the active sites and thereby decreasing the corrosion rate. The selection of a suitable inhibitor for a particular system is a difficult task because of the selectivity of the inhibitors and wide variety of corrosive environment. The choice of the inhibitors was based on the fact that these compounds contain electrons and heteroatoms such as N, O and S, which cause greater adsorption of the inhibitor molecules onto the surface of metal. It has been observed that the adsorption of corrosion inhibitors depends mainly on certain physico-chemical properties of the molecule such as functional

groups, steric factors, aromaticity, electron density of the donor atoms and p orbital character of donating electrons and also on the electronic structure of the molecules [4].

In the preliminary study corrosion tests were performed with 13Cr L80, L80, N80 and P110 steels, in order to evaluate the corrosion rate of these metals when exposed to 15% HCl acid solutions and found that corrosion rate is more for 13Cr L80 steel as shown in Table 1. So in the present work, the inhibitive action of thiophene methanol (TML) on the corrosion behaviour of 13Cr L80 steel in 15% HCl solution was investigated at different levels of concentrations (0-100 mM) using weight-loss, potentiodynamic and AC impedance spectroscopic methods. FT-IR spectral studies with the metal surface products in the presence of TML were carried out to characterize the surface products responsible for the corrosion protection. The thermal stability of the metal surface products was tested by TGA. The SEM micrographs of the metal surface in uninhibited and inhibited acid at different magnifications have been recorded to understand the surface morphology.

2 Materials and methods

2.1 Materials and medium

13Cr L80 steel samples of chemical composition given in Table 1 were used in the rectangular form of size 6.0 cm x 2.0 cm x 0.3 cm for weight-loss measurements. For electrochemical measurements the working steel specimen is covered by epoxy resin so that its cross sectional area, approximately 1 cm², was in contact with the solution. The samples were polished with different emery papers, cleaned with acetone, washed with doubly distilled water and finally dried. The working corrosive solution was 15% HCl obtained by dilution of Merck AR grade hydrochloric acid with doubly distilled water. Volume of test solution was 500 ml and 200 ml, respectively for weight-loss and electrochemical methods. All experiments were carried out in triplicate and the average values were used in corrosion rate calculations. The corrosion experiments were carried out as per the standard experimental procedures of corrosion testing [5]. Tafel and EIS experiments were carried out using EC-LAB V10.3, VMP-300 multichannel potentiostat.

Table 1: Composition* of the metals supplied by Oil & Natural Gas Commission, India and the corrosion rate (CR) in uninhibited acid.

Name of the Metal	Alloying elements (in wt.%)								CR (mm y ⁻¹)
	Fe	Cr	Mn	Si	C	Ni	P	S	
13Cr L80 steel	remainder	13.4	0.428	0.316	0.187	0.134	0.014	0.0022	44.89
L80 steel	remainder	0.190	1.41	0.353	0.263	0.159	0.03	0.001	19.20
N80 steel	remainder	0.21	1.03	0.18	0.318	--	0.017	0.014	22.86
P110 steel	remainder	--	0.71	--	0.16	--	0.002	--	29.87

* Analyzed in M/S Serval Engineers Pvt Ltd, Mangalore, India

2.2 Weight-loss method.

Cleaned and weighed 13Cr L80 steel samples were completely immersed in a beaker using glass hooks. After 6 hours of immersion, samples were withdrawn, cleaned and rinsed with doubly distilled water, washed with acetone, dried and weighed. Corrosion rate (CR) was calculated using the equation:

$$CR(mm.y^{-1}) = \frac{87.6 \times \Delta W}{DA t} \quad \text{----- (1)}$$

where t is the exposure time in hours, ΔW is the weight-loss in mg, A is the area of test coupon in cm², and D is the density of sample in gm cm⁻³. The degree of surface coverage (θ) was calculated from the weight-loss value using the equation:

$$\theta = \frac{[\Delta W_{blank} - \Delta W_{inh.}]}{\Delta W_{blank}} \quad \text{----- (2)}$$

where ΔW_{blank} is the weight-loss of steel coupon in the inhibitor-free acid and ΔW_{inh} is the weight-loss of steel coupon in the presence of the inhibitor. The experiments from normal temperature to 70 °C were carried out at constant temperature ± 0.5 °C using a calibrated thermostat.

2.3 Tafel polarization and electrochemical impedance spectroscopic (EIS) studies.

For the electrochemical corrosion measurement the arrangement used was a conventional three-electrode glass cell with a platinum counter electrode and a saturated calomel electrode (SCE) as reference. The potentiodynamic current – potential curves were recorded by changing the electrode potential automatically from -250 mV to +250 mV vs. OCP with scan rate of 1 mV s⁻¹ and the corresponding corrosion current i values, were recorded. From E vs. log i plot, E_{corr} and i_{corr} were determined. The corrosion rate (CR) was calculated using the relation:

$$CR(mm.y^{-1}) = \frac{K \times i_{corr} \times Eq.wt.}{density} \quad (3)$$

where K is 3272, a constant that defines the unit for the corrosion rate, i_{corr} is current density in $A\ cm^{-2}$ and density is in $g\ cm^{-3}$.

The surface coverage θ was calculated as:

$$\theta = \left[\frac{i_{corr(uninh)} - i_{corr(inh)}}{i_{corr(uninh)}} \right] \quad (4)$$

The percentage protection efficiency (%P) is given by

$$\%P = \theta \times 100 \quad (5)$$

The corrosion rate for all the above conditions were also obtained from EIS technique. EIS measurements were carried out in a frequency range of 1,00,000 Hz to 0.05 Hz using AC signal with an amplitude of 10 mV peak to peak at the open circuit potential. The corrosion current density i_{corr} was calculated using the charge transfer resistance (R_{ct}) together with Stern–Geary equation.

$$i_{corr} = \frac{\beta_a \times \beta_c}{[2.303R_{ct}A(\beta_a + \beta_c)]} \quad (6)$$

where A is the electrode geometric surface area and β_a and β_c are the Tafel slopes of the anodic and cathodic processes, respectively. R_{ct} value was obtained from Nyquist plot. The percentage protection efficiency, %P, was calculated from the following equation:

$$\%P = \frac{\left(\frac{1}{R_{ct}}\right)_0 - \left(\frac{1}{R_{ct}}\right)}{\left(\frac{1}{R_{ct}}\right)_0} \times 100 \quad (7)$$

where $(R_{ct})_0$ and (R_{ct}) are the uninhibited and inhibited charge transfer resistances, respectively.

2.4 Scanning electron microscopic (SEM) studies.

Surface morphology of 13Cr L80 steel samples in the acidic solutions in the presence and absence of optimal concentration of the inhibitor was performed using SEM. Immediately after the corrosion tests, the samples were subjected to SEM studies to know the surface conditions using SEM Jeol JSM-6380 LA model.

2.5 FT-IR and thermal studies of corrosion products.

Fourier Transform Infrared Spectroscopic analysis was performed on the surface products deposited on the metal surface in the presence of optimum concentration of the inhibitor at room temperature using Bruker Optik, GmbH, Tensor 27, and Opos Version 6.5 by KBr pellet technique. Thermal stability of the inhibitor and the compounds formed on the metal surface after 6 hour exposure in the acid in the presence of TML at room temperature was examined using TG/DTA 6300 (EXSTAR 6000).

3 Results and discussion

3.1 Corrosion measurement.

The results obtained from weight-loss experiments are given in Table 2. The Fig. 2 represents the variation of inhibition efficiency (η) against concentration (C). The results indicate that the 13Cr L80 steel in the absence of inhibitor corrodes severely in 15% HCl solution, while the presence of the inhibitor brings down the corrosion rate considerably. In the preliminary tests, it was found that corrosion rate (CR) of 13Cr L80 steel was maximum ($44.89\ mm\ y^{-1}$) and that of L80 steel was minimum ($19.20\ mm\ y^{-1}$) in 15% HCl medium (Table 1) among the four metal samples supplied by ONGC. High corrosion rate (CR) for 13Cr L80 steel is due to the fact that the hydrochloric acid promotes the dissolution of passivating chromium oxide film on 13Cr L80 steel (Fig. 1). The dissolution rate of the 13Cr L 80 steel in the absence of inhibitor was found to decrease non-linearly with time and the inhibition efficiency of TML was found to increase (87.48% at 24 hour exposure period) as shown in Table 3 & Fig. 3.

It is necessary to determine empirically which isotherm fits best to the adsorption of inhibitor on the steel surface. Several adsorption isotherms (viz.; Frumkin, Langmuir, Temkin, Freundlich) were tested and the Langmuir adsorption isotherm was found to provide the best description of the adsorption behaviour of TML. The Langmuir isotherm is given by following equation [6]:

$$\frac{\theta}{1-\theta} = K_{ads}C_{inh} \quad (8)$$

$$\frac{C_{inh}}{\theta} = \frac{1}{K_{ads}} + C_{inh} \text{-----} \quad (9)$$

where C_{inh} is the concentration of inhibitor, K_{ads} is the equilibrium constant of the adsorption process, and θ is the degree of surface coverage. Plot C_{inh}/θ versus C_{inh} yield a straight line with value of regression coefficient (R^2) (0.99289) almost equal to 1. This suggests that TML in the present study obeyed the Langmuir isotherm.

The data obtained suggest that TML get adsorbed on the steel surface at all temperatures studied and corrosion rates increased in the presence and absence of inhibitor with increase in temperature. In acidic media, corrosion of metal is generally accompanied with the evolution of H_2 gas; rise in temperature usually accelerates the corrosion reactions which results in higher dissolution rate of the metal. As shown in Table 4 corrosion rate increased with increasing temperature both in uninhibited and inhibited solutions while the inhibition efficiency of TML decreased with temperature and offered 77% inhibition at 70 °C (Fig. 4). A decrease in inhibition efficiency with the increase of temperature in the presence of TML might be due to weakening of physical adsorption [7, 8].

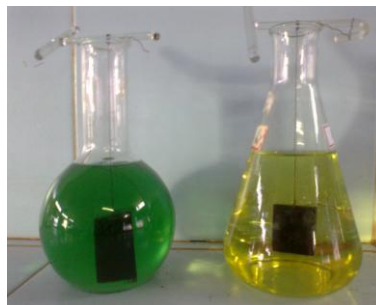


Figure 1: The photographs of 13Cr L80 and L80 samples respectively from left to right dipped in inhibitor-free 15% HCl solution after 6 hours of exposure.

Table 2: Corrosion rate (CR) and inhibition efficiency (η) for 13Cr L80 steel in 15% HCl solution inhibited by different concentrations of TML at room temperature (31 °C).

Inhibitor (mM)	CR(mm y ⁻¹)	Inhibition efficiency (η in %)
Nil	44.89	--
10	21.39	52.35
20	19.41	56.76
30	15.75	64.91
40	8.54	80.98
50	6.98	84.45
60	6.46	85.61
70	5.98	86.68
75	5.93	86.79
80	6.01	86.61
85	6.06	86.39
90	5.99	86.66
95	6.03	86.46
100	5.96	86.72

Table 3: Corrosion rate (CR) and inhibition efficiency (η) for 13Cr L80 steel in 15% HCl solution inhibited by optimum concentration of TML at different exposure periods at room temperature (31 °C).

Exposure period (h)	CR (mm y ⁻¹)		Inhibition efficiency (η in %)
	Blank	TML	
6	44.89	5.93	86.79
12	39.75	4.52	88.63
18	36.21	4.12	88.62
24	35.62	4.46	87.48

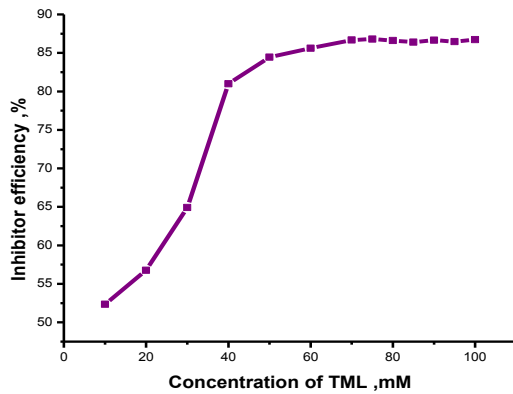


Figure 2: Variation of Inhibition efficiency with concentration of TML for 13 Cr L80 steel.

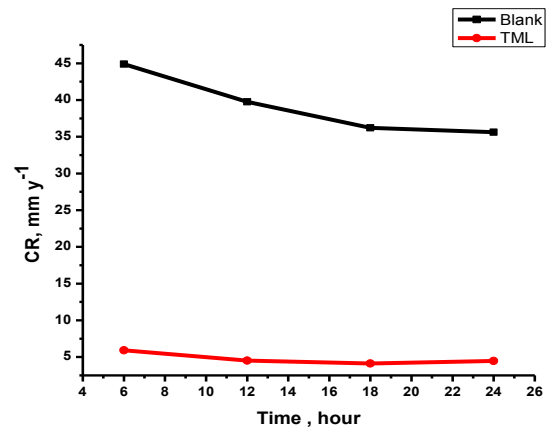


Figure 3: Variation of Corrosion rate (CR) with exposure period for 13Cr L80 steel in 15% HCl solution in the presence and absence of optimum concentration of TML at room temperature (31 °C).

Table 4: Corrosion rate (CR) and inhibition efficiency (η) for 13Cr L80 steel in 15% HCl solution in the presence and absence of optimum concentration of TML at different temperatures.

Temperature (°C)	Blank		TML	
	CR(mm y ⁻¹)	Inhibition efficiency (η in %)	CR(mm y ⁻¹)	Inhibition efficiency (η in %)
normal	44.89	--	5.93	86.79
40	68.60	--	10.98	83.99
50	98.48	--	18.78	80.93
60	288.20	--	68.85	76.11
70	875.59	--	204.39	76.66

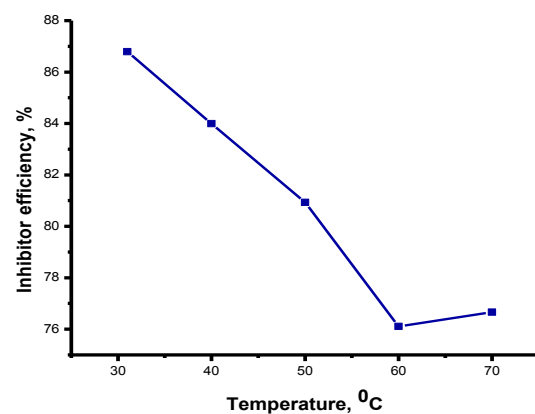
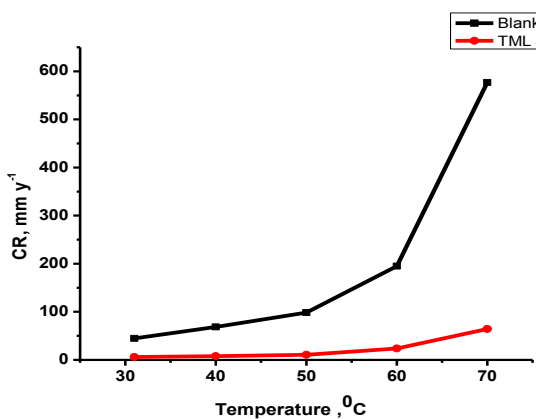


Figure 4: Variation of Corrosion rate (CR) and inhibition efficiency (η) for 13Cr L80 steel in 15% HCl solution in the presence and absence of optimum concentration of TML at different temperatures.

The Tafel curves for TML were recorded in the presence of the inhibitor at different concentrations at room temperature and are shown in Fig. 5. The maximum (97%) inhibitor efficiency is achieved at a concentration of 80 mM of TML in potentiodynamic method. The corrosion parameters obtained by using 13Cr L80 steel electrode for TML are listed in Table 6. The main impedance parameters obtained for 13Cr L80 steel in 15% HCl solution as a function of TML concentrations are listed in Table 6 together with the protection efficiency (η) derived from the impedance charge transfer of Nyquist plots (Fig. 6).

Significant reduction (upto 96%) in the corrosion rate of the sample in the inhibited acid was revealed from the reduction of i_{corr} value compared with that of the uninhibited acid solution. The E_0 value in the presence of the inhibitor shifted slightly towards negative side compared to that of inhibitor-free acid indicating that TML is acting on cathodic areas. The shift of Tafel slopes indicated that the mixed type of inhibition is offered by the inhibitor.

The semicircles in the impedance diagram indicate that the corrosion of metal is controlled by a charge transfer process. The R_{ct} values increased with the increase of inhibitor concentration indicating that more inhibitor molecule adsorb on the metal surface at higher concentration and form a surface film on the metal–solution interface. This film is formed by gradual replacement of water molecules with adsorbed inhibitor molecules, leading to an increase in the thickness of the electronic double layer and a decrease in its electrical capacitance [9]. The value of C_{dl} decreased with increasing inhibitor concentration. Decrease of C_{dl} may be caused by a reduction in local dielectric constant and/or by an increase in the thickness of the electrical double layer. These results indicate that the inhibitor act by adsorption on the metal/solution interface [9, 10, 11].

When comparing the inhibition efficiencies obtained from different testing methods, used in this study, it can be concluded that there is a fair agreement between results obtained from different techniques.

Table 5: Electrochemical corrosion parameters for 13Cr L80 steel by potentiodynamic polarization test (Tafel technique) in the presence of different concentrations of TML.

inhibitor (mM)	CR (mm y ⁻¹)	η (%)	E_0 (mV)	i_0 ($\mu\text{A cm}^{-2}$)	Tafel slopes	
					β_a (mV dec ⁻¹)	β_c (mV dec ⁻¹)
Blank	45.85	---	-428.64	4285.02	131.6	-123.5
10	5.41	88.20	-469.20	505.94	70.9	-167.3
30	4.25	90.73	-459.98	397.33	73.1	-148.7
60	3.13	93.17	-458.10	292.60	75.9	-176.3
80	1.46	96.82	-438.38	136.43	56.5	-169.5

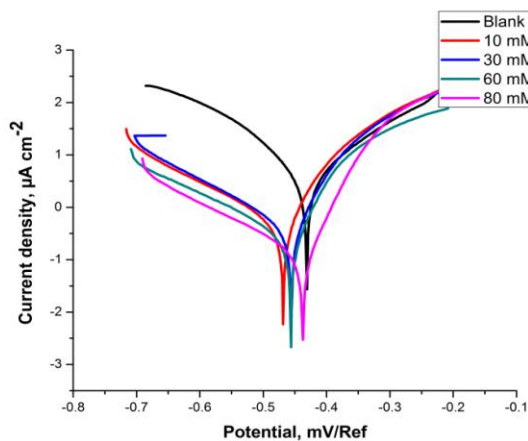


Figure 5: Tafel plots for 13 Cr L80 steel in 15% HCl in the presence of TML at different concentrations.

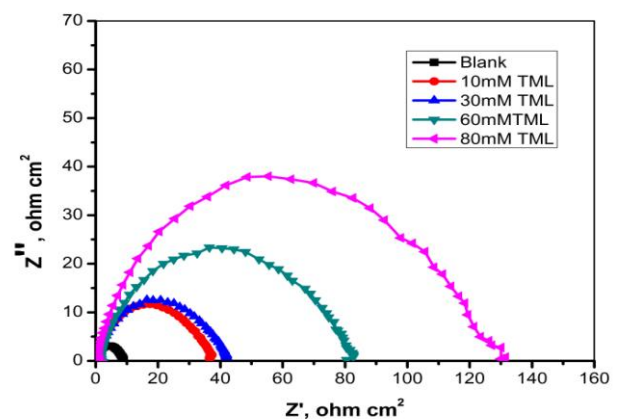


Figure 6: Nyquist plots for 13Cr L80 steel recorded in the presence of TML in 15% HCl at different concentrations.

Table 6: Electrochemical corrosion parameters for 13Cr L80 steel in the presence of different concentrations of TML by impedance method.

Concentration of inhibitor (mM)	i_{corr} ($\mu\text{A cm}^{-2}$)	CR (mm y ⁻¹)	R_{ct} (Ωcm^2)	C_{dl} ($\mu\text{F cm}^{-2}$)	%P
Blank	4046.81	43.27	8.81	360.80	---
10	647.92	6.93	37.08	67.96	76.24
30	621.22	6.64	42.29	47.45	79.17
60	355.30	3.80	81.46	49.27	89.18
80	154.54	1.65	123.00	41.08	92.84

3.2. Scanning electron microscopy.

The SEM micrograph of the specimen dipped in inhibitor-free 15% HCl solution is shown in Fig.7 (a) and reveals that severity of the corrosion attack on the metal specimen is decreased in the presence of inhibitor as shown in Fig.7 (b). The surface was free from pits and comparatively smooth. It can be concluded that corrosion was minimised in the presence of inhibitor.

3.3 FT-IR analysis and TGA result

Fig. 8 represents the merged FT-IR spectrum of pure TML and the metal surface products after 6 hour exposure in the inhibited HCl solution. The details of some of tentative assignments are given in Table 7. The peaks at 3430 and 2897 cm^{-1} observed in the spectra of the metal surface product formed in the presence of TML, may be attributed to the O-H stretching and aliphatic C-H stretching respectively (Peaks at 3342, 2931 cm^{-1} for pure TML). The characteristic sharp peaks at 840 and at 703 cm^{-1} of pure TML may be due to presence of thiophene rings. Similar sharp peaks were obtained in the case of the metal surface product at 838, 747, and 697 cm^{-1} may confirm the presence of thiophene rings [12-24]. This clearly indicates the adsorption of TML on 13Cr L80 steel was by physical forces instead of chemical combination [25].

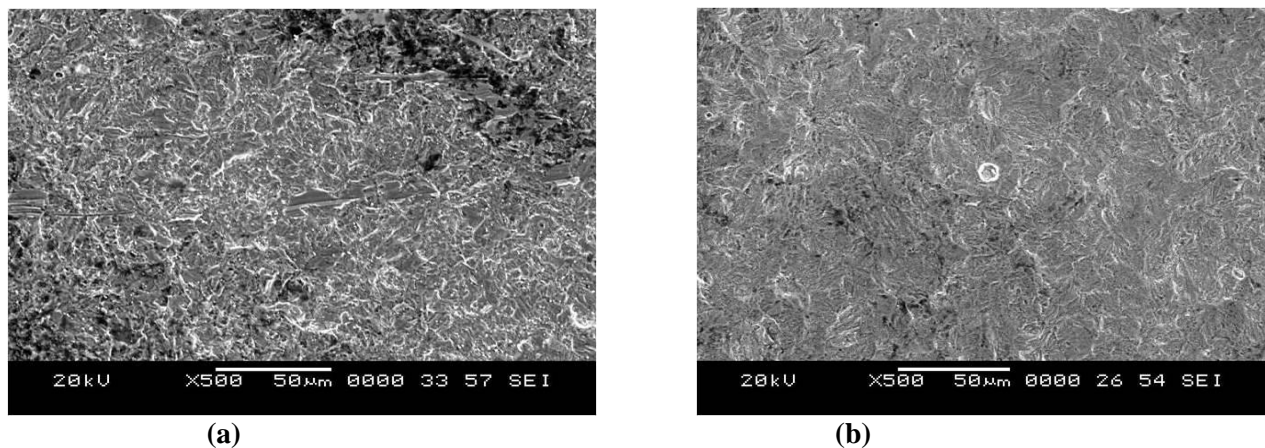


Figure 7: SEM image of the surface of 13Cr L80 steel corrosion tested in (a) uninhibited HCl solution and (b) inhibited HCl solution at room temperature.

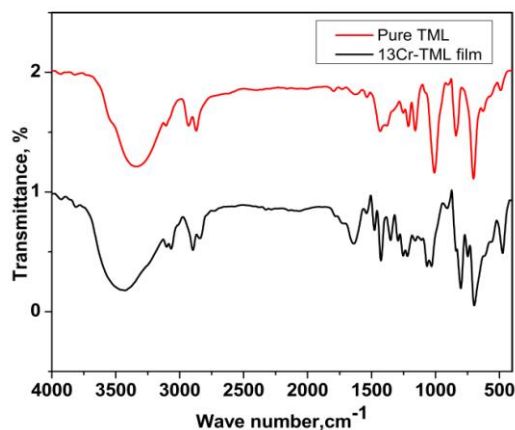


Figure 8: FT-IR spectra of pure TML and the surface product formed on 13Cr L80 steel in 15% HCl in the presence of TML.

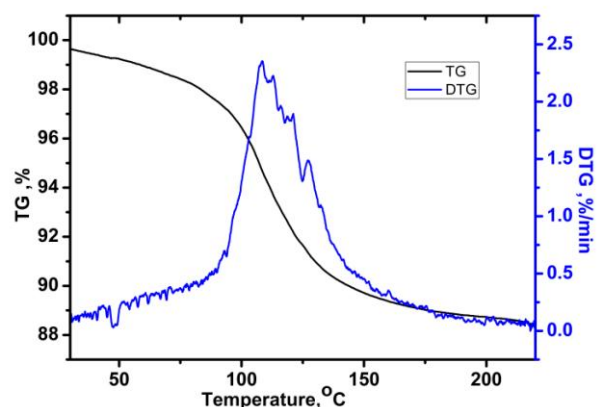


Figure 9 : TGA curve of metal surface product obtained after immersion of 13Cr L80 steel in 15% HCl acid solution containing TML.

The thermograms obtained for the surface inhibitor film, removed mechanically from the metal surface after corrosion test, are shown Fig. 9. The thermograms reveal that the initial weight-loss started very slowly that could be attributed to the volatilisation of absorbed HCl and moisture. There are sharp falls in the curve at 90-100 $^{\circ}\text{C}$ for the corrosion products which may be attributed to the degradation of the surface products formed on the

metal surface during the corrosion test. The weight-loss occurred during TGA is shown in Table 8. From the TGA it can be concluded that the surface film formed during corrosion tests are stable upto 100-140°C.

Table 7: Evaluation of the FT-IR spectrum of TML and the surface product.

Absorption frequency, cm ⁻¹ (of pure TML)	Tentative assignments	Corresponding assignments in surface product, cm ⁻¹
3342.09	O-H stretching	3430.53
3108.37		3102.59
2931.16	C-H stretching	2897.03
2871.51		2842.39
1796.59	Might be due to vibration mode of hydroxyl methyl group	-----
1730.27		-----
1626.51	Aromatic c=c stretch	1638.93
1536.6		1540
-----		1477.20
1432.28		1426.82
1252.19	Bands of deformation vibration of thiophene ring CH	1252.83
1212.14		1219.63
1158.51	C-O stretch	1158.62
1008.68		-----
903.02	Outer deformation of thiophene ring C-H	908.49
840.04		838.51
703.10		747.75
627.63	Deformation vibration of thiophene ring	697.46
490.68		475.25
-----	Might be due to the formation of iron oxide complexes	1066.51 (new peak)
-----	Might be due to the formation of iron oxide complexes	1030.94 (new peak)

Table 8: Thermogravimetric analysis

Material tested	Temperature (°C)	% age weight reduction
13Cr L80 –TML surface product after corrosion test	110	5
	200	11

3.4 Kinetic /thermodynamic studies.

To assess the influence of temperature, experiments were performed at 304 - 343°K in uninhibited and inhibited solutions containing optimum concentration of inhibitor and the corrosion rate was evaluated. The rate of increase of metal loss in the presence of inhibitor is much less than that of the inhibitor-free acid. The relationship between the corrosion rate (k) of 13Cr L80 steel in acidic media and temperature (T) is expressed by Arrhenius equation [26, 27]:

$$\log k = \frac{-E_a}{2.303RT} + \log \lambda \text{ ----- (10)}$$

where, E_a is the apparent effective activation energy, R molar gas constant and λ the Arrhenius pre-exponential factor. A plot of log of corrosion rate (k) obtained by weight loss measurement versus 1/T gives a straight line with regression coefficient close to unity. The value of apparent activation energy (E_a) has been calculated from the slope -E_a/2.303R of the obtained straight lines in the case of both inhibitor-free acid and in the presence of TML and is shown in Table 7. The increase in the apparent activation energy may be interpreted as physical adsorption that occurs in the first stage. The increase in activation energy can be attributed to an appreciable decrease in the adsorption of the inhibitor on the steel surface with increase in temperature. As adsorption decreases, more desorption of inhibitor occur because these two opposite processes are in equilibrium. Due to

more desorption of inhibitor molecules at higher temperatures the greater surface area of steel comes in contact with aggressive environment, resulting increased corrosion rates with increase in temperature [8, 28].

The values of free energy of adsorption, ΔG_{ads} , can be obtained from the following relationship

$$k_{eq} = \frac{1}{55.5} \exp\left[\frac{-\Delta G_{ads}}{RT}\right] \text{----- (11)}$$

By plotting $\log k_{eq}$ against $1/T$, the values ΔG_{ads} were calculated using the equation.

$$\Delta G_{ads} = -2.303 \times R \times \text{slope} \text{----- (12)}$$

Other kinetic parameters such as enthalpy (ΔH^*) and entropy (ΔS^*) of activation of the corrosion process may be evaluated from the effect of temperature. An alternative formula for the Arrhenius equation is the transition state equation [10].

$$k = \frac{RT}{Nh} \exp\left[\frac{\Delta S^*}{R}\right] \exp\left[-\frac{\Delta H^*}{RT}\right] \text{----- (13)}$$

where, h is the Planck's constant, N , the Avogadro's number, ΔS^* , the apparent entropy of activation and ΔH^* , the enthalpy of activation. From the plot of $\log (k/T)$ against $1/T$, ΔS^* and ΔH^* have been calculated from the intercept and slope using the following relationship.

$$\text{Intercept} = \log\left[\frac{R}{Nh}\right] + \frac{\Delta S^*}{2.303R} \text{----- (14)}$$

$$\text{Slope} = \frac{-\Delta H^*}{2.303R} \text{----- (15)}$$

Table 9: Thermodynamic and activation parameters of TML in 15% HCl solution for 13Cr L80 steel.

Inhibitor	E_a (kJ mol ⁻¹)	ΔG_{ads} kJ mol ⁻¹	ΔS^* J mol ⁻¹	ΔH^* kJ mol ⁻¹
Blank	64.608	-----	-11.907	61.937
TML	78.2003	-16.649	16.277	75.533

The negative value of ΔG_{ads} ensures the spontaneity of adsorption process and stability of the adsorbed layer on the 13Cr L80 steel surface [10, 28, and 29]. The calculated values of ΔG_{ads} for TML shown in Table 9 indicate that the adsorption mechanism of TML on 13Cr L80 steel surface involves physisorption since values of up to -20 kJ mol⁻¹ are consistent with electrostatic interaction between charged molecules and a charged metal which indicates physisorption. The positive value of enthalpy of activation (ΔH^*) in the absence and presence of inhibitor reflects the endothermic nature of 13Cr L80 steel dissolution process meaning that dissolution of steel is difficult. The value of (ΔH^*) is higher in the presence of the TML than the uninhibited solution indicating higher protection efficiency [30]. This may be attributed to the presence of an energy barrier for the reaction; hence the process of adsorption of inhibitor leads to rise in enthalpy of the corrosion process. On comparing the values of the entropy of activation (ΔS^*) shown in Table 9, it is clear that entropy of activation increased in the presence of the TML compared to free acid solution.

Conclusions

- Corrosion rate of 13Cr L80 steel is substantial in 15% HCl solution and TML shows a moderate inhibitor performance.
- Inhibition efficiency increased with an increase in TML concentration and reached 87% at 75 mM concentration at room temperature, but increased with longer exposure time. The inhibitor efficiency decreased with rise in temperature.
- The adsorption of TML on metal surface obeyed the Langmuir adsorption isotherm.
- The negative values of G_{ads} indicate that the adsorption of TML is a spontaneous process and an adsorption mechanism is typical of physisorption.
- TML is preferentially acting on cathodic areas. The shift of the Tafel slopes indicated the mixed type of inhibition was offered by TML.
- FT-IR spectral study revealed the presence of the inhibitor molecules on the metal surface product after exposure in the inhibited acid solution. This clearly indicates the adsorption of TML on the adsorbent by physical forces instead of chemical combination.
- TGA study revealed that the surface products obtained from metal surface are thermally stable up to 140 °C.

References

1. Selles C., Benali O., Tabti B., Larabi L., Harek Y., *J. Mater. Environ. Sci.* 3 (2012) 206
2. Ramananda Singh, M., Gurmeet Singh, *J. Mater. Environ. Sci.* 3 (2012) 698.
3. Menezes, M.A.M., Valle, M.L.M., Duleck, J., Neto Queiroz, J.C., *Brazilian J. of Petroleum and Gas* 1(2007) 8.
4. Khamis, E., *Corrosion* 46 (1990) 476.
5. Ailor, W.H., Hand book on corrosion testing and evaluation, *John Wiley & Sons* (1971) 119.
6. Subir Paul, Bikash Kar., *International Scholarly Research Network (ISRN) Corrosion* (2012)1, Article ID 641386.
7. Okafor P.C., Liu C.B., Liu X., Zheng Y.G., Wang F., Lin C.Y., *J. Solid State Electrochem.* 14 (2009) 1367.
8. Rekkab S., Zarrok H., Salghi R., Zarrouk, A., Bazzi, Lh., Hammouti, B., Kabouche, Z., Touzani, R., Zougagh M., *J. Mater. Environ. Sci.* 3 (2012) 613.
9. Heakal El-Taib F., Fouda A.S., Radwan, M.S., *Int. J. Electrochemical Science* 6 (2011) 3140.
10. Shukla Sudhish K., Ebenso, E. E., *Int. J. Electrochemical Science* 6 (2011) 3277.
11. Belkhaouda M., Bammou, L., Salghai, R., Benali, O., Zarrouk, A., Ebenso, E. E., Hammouti, B., *J. Mater. Environ. Sci.* 4 (2013)1042.
12. Deborah Stoner-Ma, Jaye Andrew, A., Pavel Matousek, Michael Towrie, Stephen, R. M., Peter T.J., *J. Am. Chem. Soc.* 127(2005) 2864.
13. Belobrzeckaja Costa, L., Del Boghi, M., Deluchi, G., Fumagalli, M., Drachev, A., Gilman, A., (A technical report) <http://www.isuct.ru/istapc2008/PROC/3-2.PDF>.
14. Spectroscopy data tables, infrared tables (short summary of common absorption frequencies), (A technical report) http://www.csupomona.edu/~psbeauchamp/pdf/424_spectra_tables.pdf
15. Vito Librando, Zellica Minniti, Salvatore Lorusso, *Conservation science in cultural heritage* 11(2011) 249.
16. Huang Renhe, Gao Hongmei, Tang Yaoji, Liu Qingyun, *Research & Development* 8 (2011)161.
17. Qiao Tian, Yan Chao Yuan, Min Zhi Rong, Ming Qiu Zhang, *J. of Materials Chemistry* 19 (2009)1.
18. Gopakumar B., Narayanaswamy, *Romanian J. Biophysics* 18 (2008) 217.
19. Fujil, S., Osawa, Y., Suginaira, H., *Fuel* 49 (1970) 68.
20. Bellamy, L.J., Infrared spectra of complex molecules, *Chapman Hall, London* (1975).
21. Win Maw Laingoo, H., Ph. D. thesis, Washington State Univ., Material Science Program, *IJCJ.* 12 (2007) 567.
22. Maruthamuthu S., Mohanan, S., Rajasekar, A., Muthukumar, N., Ponmarippan, S., Subramanian, P., Palaniswamy N., *Indian J. of Chemical Technology* 12 (2005) 567.
23. Brian Smith C., Fundamentals of fourier transform infrared spectroscopy, *CRC Press, Taylor & Francis group*, Boca Raton, London (2011) 90.
24. Khedr M.G.A., Lashien, A.M.S., *Corros. Sci.* 33 (1992) 137.
25. Vijayakumar G., Tamilarasan, R., Dharmendirakumar, M., *J. Mater. Environ. Sci.* 3 (2012) 157.
26. Solomon M.M., Umoren, S.A., Udousoro, I.I., Udoh, A., *Corros. Sci.* 52 (2010) 1317.
27. Gopi D., Bhuvaneshwaran, N., Rajeswari, S., Ramadas, K., *Anti-corros. Meth. Mat.* 47 (2003) 332.
28. Fouda A.S., Elewady, G.Y., El-Haddad, M.N., *Can. J. Sci. Ind. Res.*, 2 (2011) 1.
29. Ebenso E.E., *Int. J. Electrochem. Sci.* 5 (2010) 2012.
30. Ashok Kumar S.L., Iniyavan, P., Saravana Kumar, M., Sreekanth, A., *J. Mater. Environ. Sci.* 3 (2012) 670.

(2014); <http://www.jmaterenvironsci.com>